Distinguishing the effect of surface passivation from the effect of size on the photonic and electronic behavior of porous silicon

L. K. Pan, Chang Q. Sun,[a] G. Q. Yu, Q. Y. Zhang, Y. Q. Fu, and B. K. Tay
School of Electrical and Electronic Engineering, Nanyang Technological University, Singapore 639798, Singapore

(Received 19 November 2003; accepted 4 May 2004)

CF_4 plasma-passivation enhanced size dependence of the blueshift in photoemission and photoabsorption, E_{2p}-level shift, and band-gap expansion of porous silicon has been measured and analyzed numerically based on the recent "bond order-length-strength" correlation [C. Q. Sun, Phys. Rev. B **69**, 045105 (2004)]. Matching predictions to the measurements conducted before and after fluorination reveals that fluorination further enhances both the crystal binding intensity that determines the band gap and core level shift and the electron-phonon coupling that contributes to the energies of photoemission and photoabsorption. This approach enables us to discriminate the effect of surface-bond contraction from the effect of surface-bond nature alteration on the unusual behavior of photons, phonons, and electrons in nanosolid Si. © *2004 American Institute of Physics*. [DOI: 10.1063/1.1766086]

I. INTRODUCTION

It is fascinating that the structural miniaturization of solid silicon results in the blueshift in photoemission (PL) (Refs. 1 and 2) photoabsorption (PA) (Ref. 3) and the Stokes shift from the PA to the PL peak energies.[4] The size reduction also shifts the core-level energy up[5,6] and lowers the dielectric constant[7,8] of the solid silicon. The tunability of these properties has enormous impact on practical applications. There have been numerous models for the mechanisms behind these property changes from various perspectives. The most outstanding models include the "quantum confinement" theory[9] for the PL blueshift, the "initial-final state" model[6] for the core-level shift, and the Penn's model[8] for the dielectric suppression. However, consistent insight into the size-dependent change of these properties for nanosolid silicon is still lacking and a model that unifies these size-induced property changes is highly desirable. Here we show that all these changes arise from the crystal binding and electron-phonon coupling and both of which are modified by the coordination number (CN) imperfection of atoms in the surface region. We found that chemical passivation by surface fluorination that alternates the nature of the surface bond enhances the size effect. Practice and findings provide an effective way of discriminating the contribution of surface-bond relaxation from the contribution of surface-bond nature alteration to the crystal binding and electron-phonon coupling in porous silicon (p-Si).

II. MODEL

A. Bond Order-Length-Strength (BOLS) correlation versus crystal binding

The BOLS correlation premise[1,3,10,11] indicates that atomic CN imperfection results in the remaining bonds of the lower-coordinated atoms to contract spontaneously with an association of magnitude increase of the bond energy. The BOLS correlation and the lower-coordinated atoms at the curved surface of a nanosolid contribute not only to the system Hamiltonian that determines the electronic structures of the nanometric system, but also to the Gibbs free energy that determines the thermodynamic behaviors of a nanosolid. The developed premise has been successfully applied to the size-induced blueshift in the PL,[1] PA, and their energy difference, known as Stokes shift.[3] The BOLS correlation has also enabled us to estimate the single level energy of an isolated atom and its shift upon bulk formation by simulating the size dependence of the core-level shift of various specimens.[12] However, when chemical reaction occurs at the surface, the measured quantities such as the band-gap expansion, Stokes shift, and Si-2p core level shift will change further, as charge transport and bond nature alteration are involved in the reaction.[13] Practice[14–17] revealed that the effect of crystallite size (D) reduction and the effect of surface passivation enhance each other on the properties of nanometric semiconductors by perturbing the overall potential in the Hamiltonian of an extended solid, which gives rise to the corresponding expression for the band-gap expansion and the core-level shift in the form[5]

$$V(D) = V_{atom}(r) + V_{cry}(r)[1 + \delta_{surf}],$$

$$\frac{E_G(D) - E_G(\infty)}{E_G(\infty)} = \frac{E_\nu(D) - E_\nu(\infty)}{E_\nu(\infty) - E_\nu(1)} = \delta_{surf}. \quad (1)$$

The intra-atomic trapping potential $V_{atom}(r)$ defines the core-level position of an isolated atom $E_\nu(1)$. ν is an arbitrary quantum number denoting the energy level of the core electron. The crystal potential of an extended solid $V_{cry}(r)$ defines not only the band gap E_G but also the shift of the core-level energy away from the original position, $E_\nu(\infty) - E_\nu(1)$. δ_{surf} being independent of the particular form of the

[a]FAX: 65 6792 0415; Electronic mail: ecqsun@ntu.edu.sg; http://www.ntu.edu.sg/home/ecqsun/

interatomic potential is the contribution from the binding energy density rise in the relaxed region:[1]

$$\delta_{surf} = \sum_{i \leqslant 3} \gamma_i (c_i^{-m} - 1),$$

$$\gamma_i = \frac{N_i}{N} \cong \frac{\tau c_i}{K}, \tag{2}$$

$$c_i = d_i/d = 2/\{1 + \exp[(12 - z_i)/(8z_i)]\}.$$

γ_i is the portion of atoms in the ith atomic layer (N_i) compared to the total number (N) of atoms of the entire solid of different dimensionality ($\tau = 1, 2$, and 3 correspond to the dimensionality of a thin plate, a rod, and a spherical dot). $K = D/2d$ is the number of atoms lined along the radius of a spherical dot. $d = 0.2632$ nm is the diameter of a Si atom. i is counted up to three from the outmost atomic layer to the center of the solid. $c_i^{-m} = \varepsilon_i/\varepsilon_0$ describes the magnitude rise of a single bond energy upon bond relaxation. The BOLS coefficient m being an adjustable parameter, varies with the nature of the bond. z_i is the effective CN of an atom in the ith atomic layer and $z_1 = 4(1 - 0.75/k)$,[5] $z_2 = 6$, and $z_3 = 12$ worked well for a spherical dot of any size.

B. BOLS correlation versus electron-phonon coupling

The effect of electron-phonon coupling and crystal binding on the PL and PA energies[18] for porous Si has been presented in the previous work.[3] The blueshift in the PL and the PA energies are joint contribution from crystal binding and electron-phonon coupling and they can be correlated to the CN-imperfection induced bond contraction:[3,5]

$$\left.\begin{array}{l} \dfrac{E_{PL}(D) - E_{PL}(\infty)}{E_{PL}(\infty)} \\ \dfrac{E_{PA}(D) - E_{PA}(\infty)}{E_{PA}(\infty)} \end{array}\right\} = \delta_{surf} \mp B\delta_{e\text{-}p};$$

$$\delta_{e\text{-}p} = \sum_{i \leqslant 3} \gamma_i (c_i^{-2} - 1), \tag{3}$$

$$B = \frac{A}{E_G(\infty) d^2}$$

B is the e-p coupling coefficient and $\delta_{e\text{-}p}$ represents the contribution from the electron-phonon (e-p) coupling in the relaxed region. With Eq. (3) and the known $E_{PL}(\infty) \approx E_{PA}(\infty) \approx E_G(\infty) = 1.12$ eV, one can calculate the size dependence of both PL and PA energies. Simulating the measured data could define the m and the B values. For clean p-Si samples, the BOLS coefficient ($m = 4.88$), the e-p coupling coefficient ($B = 0.91$),[3,5] the $2p$-level energy of an isolated Si atom (-96.74 eV), and the crystal binding intensity (-2.46 eV) upon bulk formation[5] have been obtained with these relations.

III. EXPERIMENTAL PROCEDURES

We prepared the p-Si samples and measured the size dependence of the PL, PA, and E_{2p} peak energies before and after fluorination. Methods of fabrication of the p-Si samples are the same as described in Ref. 3. The particle size was controlled by varying the current density and estimated by matching the measured E_{PL} to the theory curve that has matched numerous sets of PL data of p-Si, CdS, and CdSe nanosolids.[1,16] Surface fluorination was performed on the p-Si samples with CF_4 plasma at room temperature by radio-frequency plasma-enhanced chemical-vapor deposition with an unparallel plate configuration. The base pressure is less than 5×10^{-5} Torr maintained by a turbomolecular pump. The p-Si samples were placed on the cathode electrode with 20 cm diameter. CF_4 gas was introduced with a flow rate of 10 sccm (SCCM denotes cubic centimeter per minute at STP) and the chamber pressure was kept at 25 mTorr. A radiofrequency power of 100 W was applied for 2 min. The F/Si ratio calculated from the area ratio of corresponded peaks in the x-ray photoemission spectroscopy (XPS) spectra is about 0.3 for all the fluorinated samples. No apparent particle-size reduction upon fluorination can be resolved using atomic force microscopy. Usually, F-plasma etching of Si or SiO_2 surface is carried out by bombarding the surface with 350 W plasma for several hours.

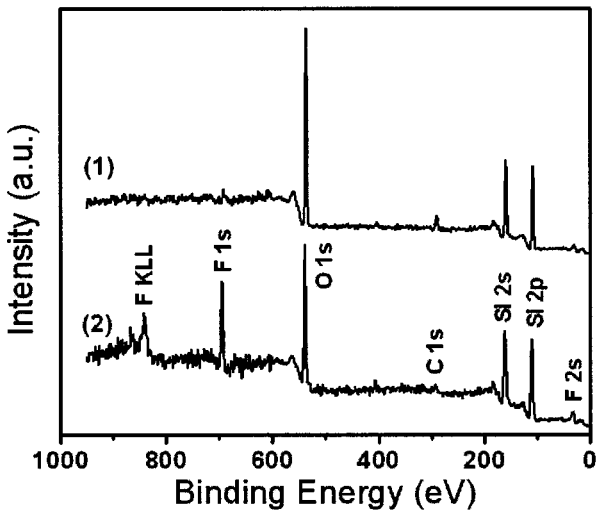

FIG. 1. XPS spectra of the p-Si sample E before (1) and after (2) fluorination. It shows the existence of fluorine in fluorinated sample.

IV. RESULTS AND DISCUSSION

Figure 1 compares the XPS spectra of the p-Si sample E (Table I) before (as grown) and after fluorination. It can be seen that besides Si and F, O and C also exist on the surface. The existence of a little fluorine in the as-grown sample can be due to HF acid remnants inside voids after preparation because only HF and SiF_6^{2-} were found using ^{19}F nuclear magnetic resonance (NMR).[19,20] Upon fluorination, surface fluorides exist in the form of SiF_2 species[21,22] which modify the chemical structure of the p-Si surface through bond reforming from Si-H bond. The source of carbon is not ethanol because the carbon amount is similar to that in samples anodized in water-HF solutions.[23] The carbon should come from hydrocarbon molecules in the ambient and often in the residual gas in analysis chambers used for XPS.[24] Oxygen exists in the form of Si-O-Si and O_x-Si-H groups on the

TABLE I. Measured E_{PL}, E_{PA}, and E_{2p} of F-passivated *p*-Si with particle size *D*.

Sample	*D*(nm)	E_{PL}(eV)	E_{PA}(eV)	$E_{2p}(D)$(eV)
A	1.4	2.28	3.15	−103.31
B	1.6	2.18	3.01	−103.06
C	1.7	2.14	2.92	−102.73
D	1.9	2.01	2.74	−102.31
E	2.1	1.89	2.43	−101.17
Bulk	∞	1.12	1.12	−99.37

p-Si surface and is normally adsorbed in a few minutes after drying in ambient. Nevertheless, coexistence of these elements may contribute to the F surface passivation. As noted in Ref. 13 that reaction with C, N, O, and F has the similar effect on the binding energy enhancement due to the charge transportation. The extent of contribution may be different due to the difference of atomic valence and also the richness of the corresponding element. From this perspective, we may treat the F plasma passivation as a resultant effect of these elements as it is not realistic to distinguish the contribution from the individual element.

Figure 2 shows PL spectra of as-grown (dash line) and fluorinated (solid line) *p*-Si samples measured under a Xe lamp ($\lambda = 458$ nm) excitation and a SPEX FLUOROLOG-3 spectrofluorometer at room temperature under ambient environment. Compared with the as-grown samples, the passivated ones exhibit a blueshift in the PL, evidencing an enhancement of crystal field due to bond nature alternation and screen weakening as well as valence charge repopulation that leaves holes behind the top of the valence band.[25] Figure 3 shows room temperature reflection spectra of (a) as-grown and (b) fluorinated *p*-Si samples that were measured using a Perkin Elmer Lamda 16 UV/VIS reflection spectrometer. The reflectivity varies with the size reduction and surface fluorination in the range of 200–900 nm, which is related to

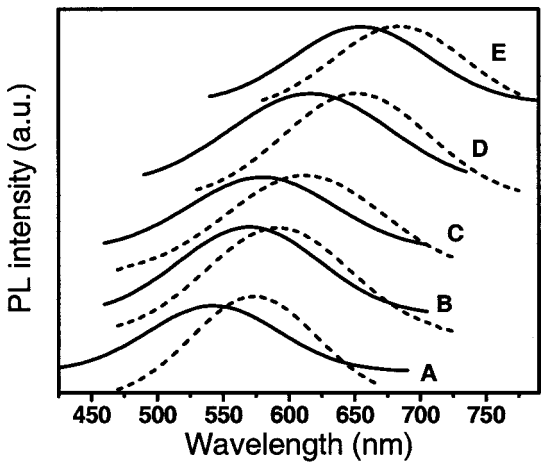

FIG. 2. Size-dependent PL spectra of as-grown (dash line) and fluorinated (solid line) *p*-Si samples. The data of sizes are given in Table I.

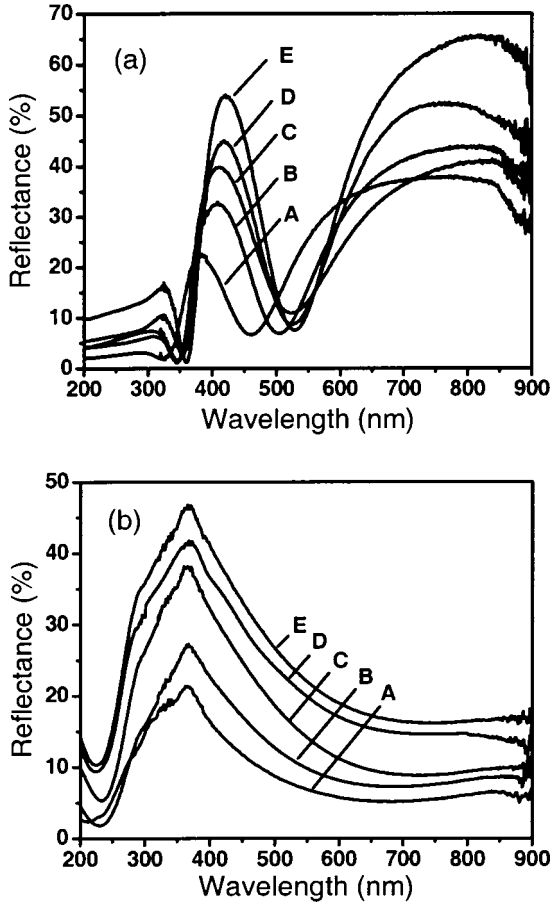

FIG. 3. Room temperature reflection spectra of (a) as-grown and (b) fluorinated *p*-Si samples.

the change of dimension and geometry of columns and voids on the *p*-Si surface. Figure 4 displays the spectral dependence of the absorption coefficient of (a) as-grown and (b) fluorinated *p*-Si samples obtained by fitting reflection spectra using the SCOUT commercial software.[26,27] As observed, the values of absorption coefficient are strongly dependent on the size and surface fluorination, especially in the range of higher photon energy. The absorption edge can be extracted from the Tauc plot deriving from the absorption spectra.[28,29] Figure 5 compares XPS Si-2*p* profiles of as-grown (dash line) and fluorinated (solid line) *p*-Si samples measured using a Kratos AXIS spectrometer with monochromatic Al $K\alpha(h\nu = 1486.71$ eV) radiation at ambient temperature. The shift of the binding energy (BE) due to charging was corrected using C1*s* binding energy (284.8 eV) from the surface C contamination. There is an obvious Si-2*p* core level shift for *p*-Si samples before and after fluorination. The mechanism responsible for this core-level shift is the same as the one for PL blueshift upon fluorination.

Matching the prediction in Eq. (3) with the experimental data on PA and PL peak energies, we can get the coefficient $B = 1.04$ and $m = 5.32$. The *B* and *m* values here are larger than the corresponding values ($B = 0.91$ and $m = 4.88$) for clean *p*-Si,[3,5] showing apparent enhancements of electron-phonon interaction and crystal binding by surface fluorination. As discussed earlier, surface chemical reaction can contribute to the crystal binding intensity, transfer electrons from

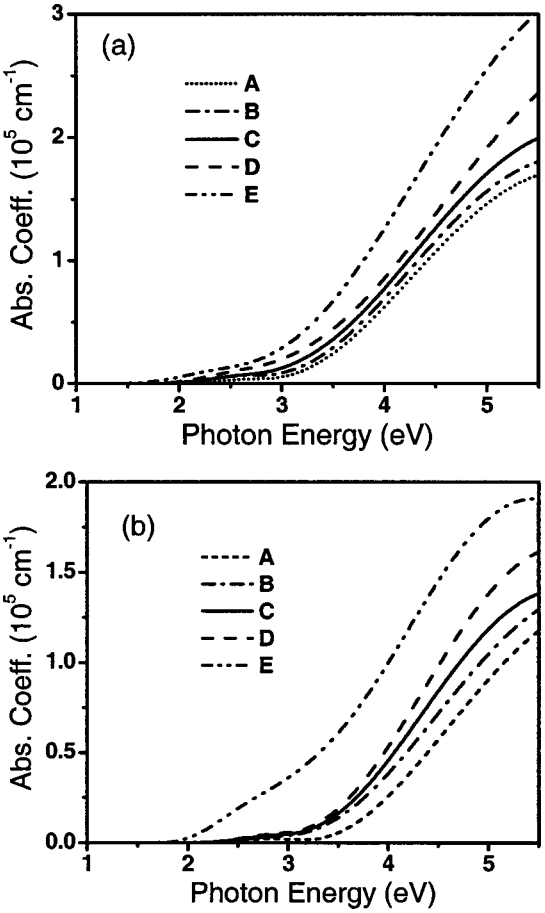

FIG. 4. Comparison of room temperature absorption spectra of (a) as-grown Ref. 4 and (b) fluorinated *p*-Si samples, from which the PA energies are derived with the Tauc plot method.

one specimen to another that causes the valence charge transportation from Si to F and thus enhance the crystal field. On the other hand, surface bond nature alteration also results in the variation of vibration frequency[10] and larger vibration amplitude of surface atoms.[30,31] The electron-phonon coupling will therefore be enhanced. Based on the BOLS coefficient $m=5.32$ and the atomic trapping energy of the $2p$ electron of an isolated Si atom $E_{2p}(1)=-96.74$ eV,[5] the bulk crystal binding intensity $\Delta E_{2p,F}(\infty)=E_{2p,F}(\infty)-E_{2p}(1)$ is

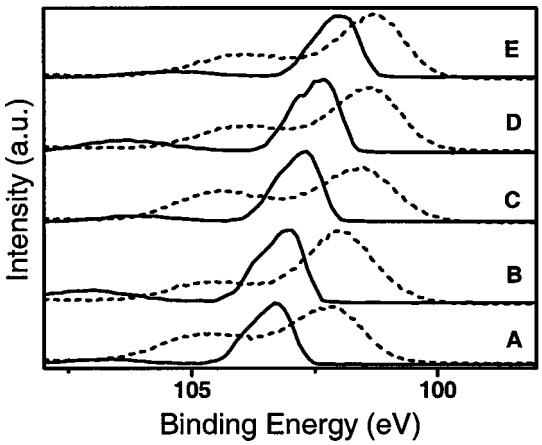

FIG. 5. Size-dependent XPS Si-$2p$ profiles of as-grown (dash line) and fluorinated (solid line) *p*-Si samples.

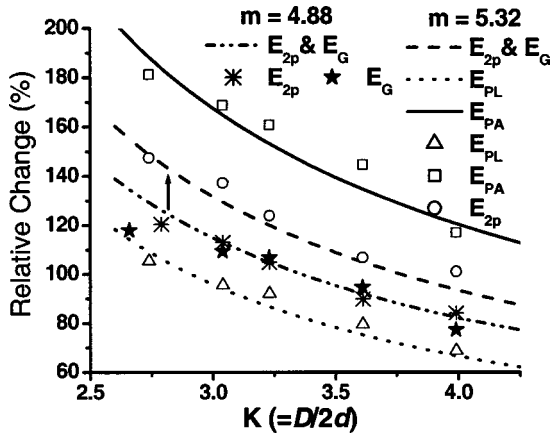

FIG. 6. Comparison of the predicted with measured PA and PL peak energies and the E_G and E_{2p} shift of clean ($m=4.88$) and fluorinated ($m=5.32$) *p*-Si. The E_{2p} and E_G data for the clean *p*-Si are from Refs. 3 and 5, respectively. The arrow indicates the flurination effect which displace the E_G and E_{2p} line up.

shifted from −2.46 to −2.63 eV. Consistency between the predicted and the experimental PA and PL blueshift and the core-level shift (band-gap expansion as well) after fluorination is given in Fig. 6. Agreement of the predicted with the observed PA, PL, and E_{2p}-shift ensures the reliability of the data obtained and evidences the validity of the BOLS correlation for nanosolid. The theoretically predicted and the measured E_{2p} and E_G for clean ($m=4.88$) *p*-Si are also compared in this figure. The effect of fluorination on the binding energy is thus easily distinguished as indicated by the vertical arrow.

V. CONCLUSION

Surface passivation by plasma fluorination with C and O contribution is found to further enhance both the crystal binding intensity by surface-bond nature alteration (from $m=4.88$ to 5.32) that determines the band-gap and core-level shift and the electron-phonon coupling (from $B=0.91$ to 1.04) that contributes to the energies of photoemission and photoabsorption of *p*-Si. The BOLS correlation enables us to unify the observed blueshift in the PL and PA, the energy shift of the Si-$2p$ core level, as well as the dielectric suppression[7] to the effect of atomic CN imperfection of atoms near the edge of surface. The BOLS also enables us to discriminate the contribution from bond relaxation and bond nature alteration to both the crystal binding and electron-phonon coupling that determine the unusual behavior of photons, phonons and electrons in *p*-Si. Practice should provide a helpful means for distinguishing the effect of surface passivation from the effect of size reduction on other size-dependent properties of other nanostructured materials.

[1] L. L. Wang and A. Zunger, Phys. Rev. Lett. **73**, 1039 (1994).
[2] L. K. Pan, C. Q. Sun, B. K. Tay, T. P. Chen, and S. Li, J. Phys. Chem. B **106**, 11725 (2002).
[3] Y. Kanemitsu, H. Uto, Y. Masumoto, T Matsumoto, T. Futagi, and H. Mimura, Phys. Rev. B **48**, 2827 (1993).
[4] L. K. Pan and C. Q. Sun, J. Appl. Phys. **95**, 3819 (2004).
[5] C. Q. Sun, L. K. Pan, Y. Q. Fu, B. K. Tay, and S. Li, J. Phys. Chem. B **107**, 5113 (2003).
[6] M. Aldén, H. L. Skriver, and B. Johansson, Phys. Rev. Lett. **71**, 2449 (1993).

[7]C. Q. Sun, X. W. Sun, B. K. Tay, S. P. Lau, H. Huang, and S. Li, J. Phys. D **34**, 2359 (2001).
[8]D. R. Penn, Phys. Rev. **128**, 2093 (1962).
[9]A. D. Yoffe, Adv. Phys. **50**, 1 (2001); **51**, 799 (2002).
[10]C. Q. Sun, S. Li, and B. K. Tay, Appl. Phys. Lett. **82**, 3568 (2003).
[11]C. Q. Sun, Y. Wang, B. K. Tay, S. Li, H. Huang, and Y. Zhang, J. Phys. Chem. B **106**, 10701 (2002).
[12]C. Q. Sun, Phys. Rev. B **69**, 045105 (2004).
[13]C. Q. Sun, Prog. Mater. Sci. **48**, 521 (2003).
[14]A. A. Fillos, S. S. Hefner, and R. Tsu, J. Vac. Sci. Technol. B **14**, 3431 (1996).
[15]S. Bayliss, Q. Zhang, and P. Harris, Appl. Surf. Sci. **102**, 390 (1996).
[16]C. Q. Sun, S. Li, B. K. Tay, and T. P. Chen, Acta Mater. **50**, 4687 (2002).
[17]W. T. Zheng, C. Q. Sun, and B. K. Tay, Solid State Commun. **128**, 381 (2003).
[18]R. A. Street, *Hydrogenated Amorphous Silicon* (Cambridge University Press, Cambridge, 1991), p. 279.
[19]B. M. Kostishko, S. V. Appolonov, and A. E. Kostishko, Appl. Surf. Sci. **189**, 113 (2002).
[20]D. Petit, J. N. Chazalviel, F. Ozanam, and F. Devreux, Appl. Phys. Lett. **70**, 191 (1997).
[21]Y. Okada, J. Chen, I. H. Campbell, P. M. Fauchet, and S. Wagner, J. Non-Cryst. Solids **114**, 816 (1989).
[22]K. Baert, P. Deschepper, J. Nijs, and R. Mertens, Appl. Phys. Lett. **60**, 442 (1992).
[23]C. Ortega, J. Siejka, and G. Vizkelethy, Nucl. Instrum. Methods Phys. Res. B **45**, 622 (1990).
[24]L. T. Canham, M. R. Houlton, W. Y. Leong, C. Pickering, and J. M. Keen, J. Appl. Phys. **70**, 422 (1991).
[25]C. Q. Sun, Appl. Phys. Lett. **72**, 1706 (1998).
[26]W. Theiss, *Scout Thin Film Analysis Software Handbook, Hard and Software* (M. Theiss, Aachen, Germany, 2001), www.mtheiss.com.
[27]W. Theiß, Surf. Sci. Rep. **29**, 91 (1997).
[28]S. Guha, P. Steiner, and W. Lang, J. Appl. Phys. **79**, 8664 (1996).
[29]S. Furukawa and T. Miyasato, Phys. Rev. B **38**, 5726 (1988).
[30]Q. Jiang, Z. Zhang, and J. C. Li, Chem. Phys. Lett. **322**, 549 (2000); F. G. Shi, J. Mater. Res. **9**, 1307 (1994).
[31]L. K. Pan, C. Q. Sun, and C. M. Li, J. Phys. Chem. B **108**, 3404 (2004).